JOURNAL OF GEOPHYSICAL RESEARCH, VOL. 102, NO. D11, PAGES 12,971–12,985, JUNE 20, 1997

Ozone diurnal variations observed by UARS and their model simulation

Frank T. Huang
Science Systems and Applications Inc., Lanham, Maryland

Carl A. Reber
NASA Goddard Space Flight Center, Greenbelt, Maryland

John Austin
U.K. Meteorological Office, Bracknell, England

Abstract. Several years of ozone measurements from the Microwave Limb Sounder onboard the Upper Atmosphere Research Satellite are analyzed using a two-dimensional Fourier series in day of year and time of day. Because of limited temporal coverage near local noon, only the diurnal and semidiurnal components are included. Data are investigated in detail at 28°N in the middle stratosphere to lower mesosphere, where the data are considered most reliable. The observations show that ozone is a maximum in the afternoon at 3 mbar and a minimum in the afternoon at 1 mbar and above with a narrow transition zone of reduced diurnal variation in between. This strong dependency on altitude in the transition from a maximum in the afternoon to a minimum in the afternoon, coupled with the small percentage changes in ozone, imposes strict requirements on the data and on the analysis of the data. Comparisons are made with results from a photochemical box model run at 11 levels between 0.46 mbar and 21.5 mbar for 28°N at spring equinox and near the solstices. This is the first time that a data analysis and model comparison of this kind has been made, leading to the identification of relatively small diurnal variations, especially in the transition zone. In the middle stratosphere the model results are in poor agreement with the observations because of the influence of stratospheric dynamics which are neglected in the model runs. In the upper stratosphere the model shows the expected underprediction of absolute ozone amounts, although the percentage change from the midnight value is in excellent agreement with the observations and in particular correctly simulates the diurnal variation in the transition zone between 3 and 1 mbar. Model sensitivity studies are performed to determine the effects of major reaction rate changes and simplified tidal effects.

1. Introduction

The investigation of diurnal variations of chemical constituents has provided one of the most challenging tests of photochemical theory. Many of these have concentrated on measuring the nitrogen species by balloon [e.g., *Webster et al.*, 1990; *Kondo et al.*, 1990] combined with photochemical modeling. Such studies have shown, in general, that the relatively straightforward diurnal variations in the nitrogen species are well simulated by photochemical models using currently recommended reaction rates. Diurnal variations of other species, particularly ozone, have also been measured by balloon [e.g., *Webster and May*, 1987], while ozone diurnal variations have also been measured from the ground using microwave techniques [e.g., *Zommerfelds et al.*, 1989; *Connor et al.*, 1994]. Unfortunately, these measurements have, in general, rather poor spatial coverage. Improved spatial coverage, for example, from earlier satellite data, has not significantly improved our understanding of diurnal variations as Earth-observing satellites have typically been placed in near-Sun synchronous orbits (e.g., Solar Mesosphere Explorer (SME) [*Barth et al.*, 1983, and limb infrared monitor of the stratosphere (LIMS) [*Gille and Russell*, 1984]). Studies from such data sources have therefore been restricted to the analysis of day-night differences [e.g., *Siskind et al.*, 1994] or to the mesosphere, where the diurnal variation is most marked (see *Clancy et al.* [1987] and *Bjarnason et al.* [1987] for SME measurements).

Orbital precession resulting from the 57° inclination of the Upper Atmosphere Research Satellite (UARS) orbit allows most local times to be sampled over a period of about 36 days [*Reber*, 1993, *Reber et al.*, 1993]. Data with this extent of coverage in local time and over large parts of the globe have not been available before. The UARS Microwave Limb Sounder (MLS) [*Waters*, 1993; *Barath et al.*, 1993] instrument has been providing excellent data on atmospheric temperature, ozone, and other trace species since shortly after the September 1991 launch. *Ricaud et al.* [1996] have compared the diurnal variations of MLS ozone in the mesosphere with ground-based measurements and theoretical models. This study did not attempt to distinguish variations with day of year from diurnal variations. Instead, they analyzed mesospheric data, where the day-of-year variations

Paper number 97JD00461.
0148-0227/97/97JD-00461$09.00

are expected to be small and where the diurnal variations are greater than 10%. In this paper we present a complementary study to those above, using MLS data to study ozone diurnal variations in the middle and upper stratosphere where their magnitudes may be smaller than the change from one month to the next. Sensitivity problems are thus more acute, and care must be taken to identify day-of-year variations in addition to diurnal variations. The altitude range we address is 21.5 mbar to 0.46 mbar.

Despite the many improvements in photochemical modeling in the last 10 years there have been relatively few attempts to simulate the diurnal variation of ozone since the early work of *Pallister and Tuck* [1983]. Their work concluded that investigating the diurnal variations was a useful way of testing photochemical models by looking at the relative variation during the day rather than the absolute values, which can be adversely affected by measurement accuracy. The availability of the diurnal variations from UARS provides a new opportunity to test our quantitative understanding of the photochemistry of ozone. In this work an updated version of the Pallister and Tuck model is employed and compared with UARS data for the spring equinox and near the two solstices at 28°N, thereby providing tests over the widest range of solar zenith angles permitted by the data with the techniques used here. The characteristics of UARS data are described in section 2, and in section 3 the measurements and the algorithm used to extract diurnal variations are discussed, along with selected results. Section 4 describes the photochemical model, while comparisons between model results and observations are included in section 5. Sensitivity of the model results to key reaction rates and to vertical transport is investigated in section 6, and in section 7 the results are summarized and discussed.

2. Observations

2.1. UARS Data Characteristics

The Upper Atmosphere Research Satellite (UARS) [see *Reber*, 1993; *Reber et al.*,1993] was launched by the space shuttle on September 12, 1991, into a near circular orbit at 585 km altitude inclined 57° to the equator. Measurements include solar energy inputs to the atmosphere and vertical profiles of temperature, important minor gas species, and wind fields. The orbital parameters, combined with the sensor measurement characteristics, yield an atmospheric measurement pattern that produces near-global coverage with a duty cycle that periodically favors the northern or the southern hemispheres for several of the instruments. In more than 5 years of operation, the UARS has provided an unprecedented set of unified and coordinated measurements. In particular, the UARS measurement-tracks for the atmospheric limb-sounding instruments sample most of the range of local solar times, thereby providing information on the diurnal variation of the measured parameters. Data with this type and extent of coverage in local time and with this extent of global coverage have not been available before. The data used here are level 3B (L3B) representations of MLS measurements. The L3B data are Fourier series estimates of level 3AL data around a latitude circle at standard UARS latitudes and pressure levels. We use the leading Fourier coefficient of the L3B data as the zonal mean. The MLS level 3AL data are from the version 3 production processing of ozone (205-GHz radiometer) and temperature.

2.2. Sampling Pattern

To keep the instruments from pointing directly at the Sun and to maintain thermal control, the UARS observatory is rotated by 180° about the yaw axis on an average of once every 36 days, or one "yaw period". Because the limb-sounding instruments generally view to the side of the orbital plane, the yaw also changes the instruments' view direction. As a result, the latitude coverage changes from 32°S - 80°N to 80°S - 32°N on alternate yaw periods. Therefore, poleward of plus and minus 32° latitude, data are missing on alternate yaw periods, and we cannot use the present analysis. For a given day, latitude, and mode (ascending or descending-ascending means the spacecraft is heading north at the equator), the local solar times of the measurements at the various longitudes around a fixed latitude circle decrease by only about 20 min from day to day due to the orbital precession. When both ascending and descending mode data are used, it takes about 36 days to sample 24 hours of local solar times. Because of the orbital inclination, the local time of the measurements is a strong function of their latitude, even within a given day. Figure 1a depicts the measurement geometry.

2.3. Data Gaps

There have been periods of days or weeks when the observatory has not collected data because of various spacecraft-related problems. In addition, MLS had some scanning problems beginning in 1994. Also, on and around yaw days there are either no raw data or no L3B data available. However, a few missing days causes no problems in applying the diurnal variation algorithm, but longer periods of missing data may create difficulties.

In terms of local solar time, there are data gaps around local noon, which are a natural consequence of the instrument view directions and the observatory yaws. Examples of these gaps as a function of day of year can be seen in Figure 6 and of local time in Figure 3. The size of the gaps depend on the latitude, the time of year, and the view direction of the instrument.

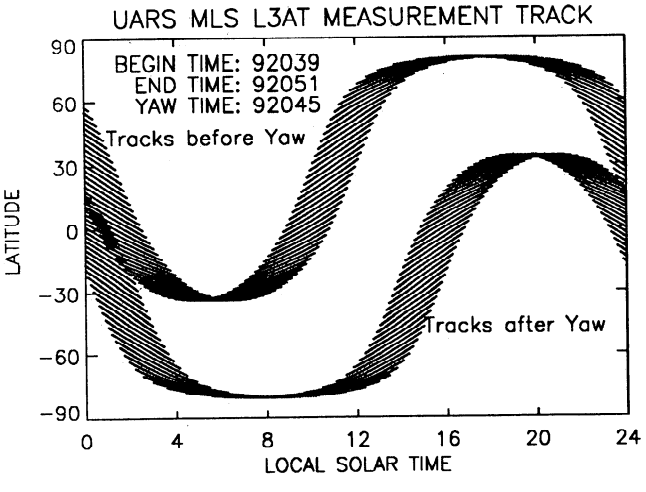

Figure 1a. Local solar time as a function of latitude for Microwave Limb Sounder (MLS) measurement tracks. The yaw day is 92045, and measurement tracks are shown for several days before and after yaw. The data along the measurement tracks at regular time intervals of 65.5 s are called level 3AT data.

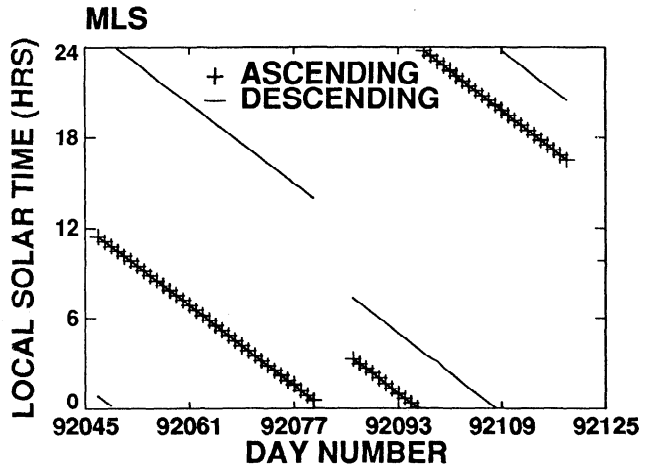

Figure 1b. Local solar time (hours) of the MLS measurement track at 28°N as a function of day-of-year during the yaw periods from year-day 92045 (February 14) to 92122 (May 1). The pluses stand for local times of data measured on ascending modes, and the line denotes those for descending modes.

3. Diurnal Variation Analysis

3.1. Measurements

For clarity, in most of the following we present and discuss data only for the year 1992. Some interannual variations are present in the data, but these are relatively small. In the following we denote the day of year by a 5-digit number YYDDD, where YY stands for the year number of the twentieth century, and DDD is the day number of the year, with January 1 being the first day.

Figure 1b shows the local solar time of the MLS measurement track at 28°N as a function of day of year over two yaw periods, from year-day 92045 to 92125. For the same period, zonal mean MLS O_3 (ppmv, from the 205-GHz channel) at 28°N and 10 mbar is also illustrated (Figure 2). It can be seen that the ascending mode (pluses) ozone mixing ratios in the first group of days are higher than in the descending mode, while the situation is reversed toward the end. This implies that the ozone values in daylight are higher than at night. We attribute the differences in the zonal means at the two local times (ascending and descending modes) sampled for a given day and a given latitude to variations with local time. It can be seen that day-of-year variations over most of the period are significantly larger than diurnal variations inferred here. On the other hand, the jump in the data near local noon (Figure 3) is primarily due to the variation with day of year and not due to diurnal variations. The two adjacent points in local time at the discontinuity near 1200 (marked by the boxed numbers 1 and 4) are measured at the beginning and end of the yaw period, respectively, and therefore are measured more than 30 days apart. Data acquired from the first half of the solar day were from the ascending portion of the orbit (boxed numbers 1 and 3), while data from local noon to midnight were measured during the descending portion (boxed numbers 2 and 4). Although annual variations are more pronounced at 10 mbar than at most other pressure levels, this example shows the necessity of separating the diurnal variations in the data from the day-of-year variations.

Figures 4a-4d correspond to Figure 2 but for the pressure levels 4.6, 2.2, 1.0, and 0.46 mbar, respectively, and cover only the earlier yaw period (from 92045 to 92083). It can be seen that at 4.6 mbar and 2.2 mbar, as in the 10 mbar case, the daylight values are generally larger than the nighttime values. At 1 mbar the situation is changing, and at 0.46 mbar the relative day-night densities have reversed. The day-to-day variations are also smaller at these lower pressures than the variations at 10 mbar.

With the aid of Figure 1b, it can be seen that between year-days 92061 and 92069, data for both the ascending and the descending modes are nightside of 1800 and 0600. During these days the zonal means for both modes were very similar and approximately constant at pressure heights of 1.0 and 0.46 mbar, indicating little ozone variation at night. At 10 mbar the ascending and descending mode measurements were also very similar, again suggesting little diurnal variation at night, but there was a drift in the values during the

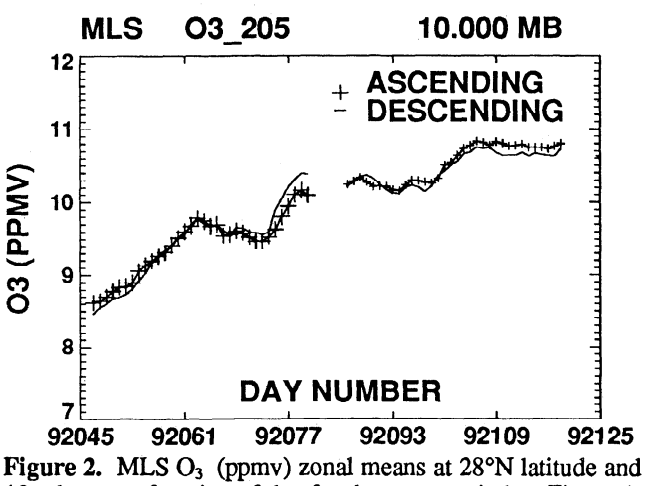

Figure 2. MLS O_3 (ppmv) zonal means at 28°N latitude and 10 mbar as a function of day for the same period as Figure 1, namely, year-days 92045 (February 14) to 92122 (May 1). The two curves are for ascending (pluses) and descending (line) mode zonal means.

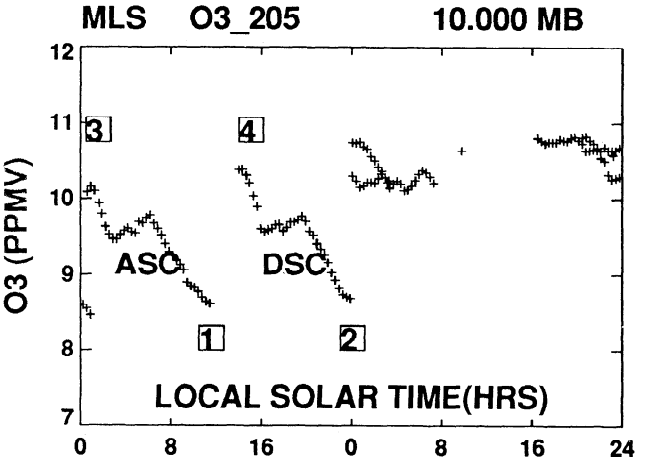

Figure 3. MLS O_3 (ppmv) corresponding to Figure 2, for year-days 92045 (February 14) to 92122 (May 1) but as a function of local time rather than day of year. For clarity, data from the two yaw periods have been offset from each other by 24 hours.

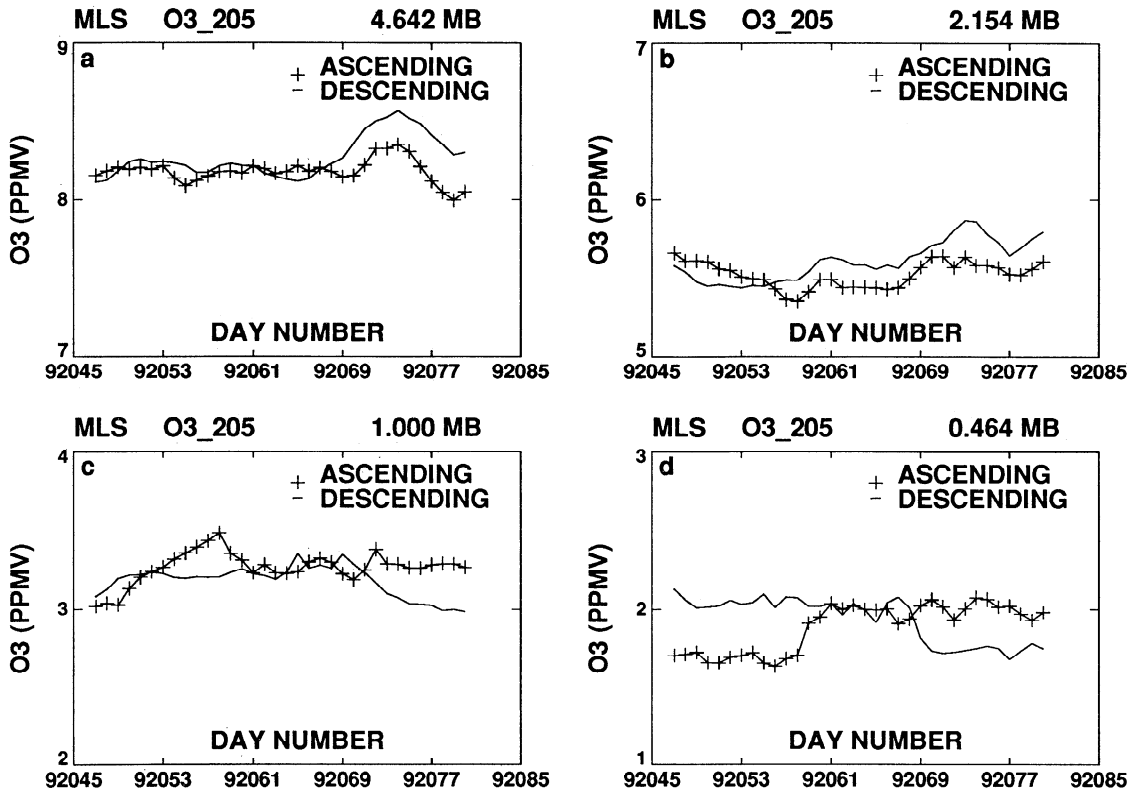

Figure 4. MLS O_3 corresponding to the first yaw period (92045 to 92085) of Figure 2 but for pressure levels (a) 4.6 mbar, (b) 2.15 mbar, (c) 1.0 mbar, and (d) 0.46 mbar.

period, possibly because of day-of-year effects. In comparison, at 2.2 mbar (Figure 4b) the values are constant during the period 92061 to 92069, but the ascending and descending modes are offset slightly. Although not shown here, data from the same period in 1993 (year-day interval 93040-93080) show qualitative agreement at these pressures, including the ascending/descending mode offset for 2.2 mbar.

3.2. Diurnal Variation Algorithm

To separate the diurnal variations from the annual (day of year) variations, we consider the data in Figure 2, plus the data for other times of the year as a time series which is a function of two variables, namely, local solar time and day of year. These zonal mean data are used to make Fourier series estimates, as represented by

$$\overline{Y}(s_i, d_k)_{\phi,z} = \sum_n \sum_m \overline{a}_{nm} e^{i\omega_n s_i} e^{i\beta_m d_k}$$

where s_i is local solar time (hours), ϕ is latitude, d_k is day number, z is pressure altitude,

$$\omega_n = 2\pi n / 24, \quad \beta_m = 2\pi m / 365,$$

and the overbars denote zonal means. The use of latitude and altitude as subscripts denotes that they are fixed in value. The indices n and m denote the wave numbers in local time and day of year respectively, and the maximum values of n and m are 2 and 10, respectively. Because it takes about 36 days to sample the range of local times, we also assume that the day-of-year variations of the diurnal and semidiurnal coefficients which are more rapid than seasonal are negligible. Therefore diurnal and semidiurnal coefficients with day-of-year wave numbers greater than 4 are assumed negligible, and are not estimated. The coefficients $\{\overline{a}_{nm}\}$ are estimated using a least squares fit, which minimizes the sum of the squares of the differences between the Fourier series and the data, similar to the discussions by *Reber et al.* [1994] and *Huang et al.* [1994].

The algorithm does not require sampling at regular, fixed intervals of day of year or of local solar time. It is also relatively tolerant of data gaps. However, inordinately large data gaps create difficulties and limit the order of the Fourier series expansion, especially when the data contain significant noise or uncertainties. Tests have shown that the algorithm can accurately retrieve test input data which consist of linear combinations of sines and cosines at the Fourier frequencies. The test input was based on actual sampling patterns in local time and day of year of the MLS measurement track for 1992. However, the algorithm (like all implementations of finite, discrete, Fourier series) is susceptible to problems such as aliasing and leakage. These problems can be caused by undersampling, the finite length of the data, the existence of frequencies in the data which are not at the Fourier frequencies, and the periodicity (or lack thereof) of the data. As used here, the term aliasing refers to all ambiguities and biases which arise due to sampling, such as undersampling or irregular sampling. Tests have shown that the algorithm does not introduce additional aliasing. Also, no attempt has been made to remove secular trends. As it turns out, the data are approximately cyclical over a one-year period, so for purposes here, trends should not be a significant problem. However, results at the beginning and end of the period under consideration may have more uncertainty.

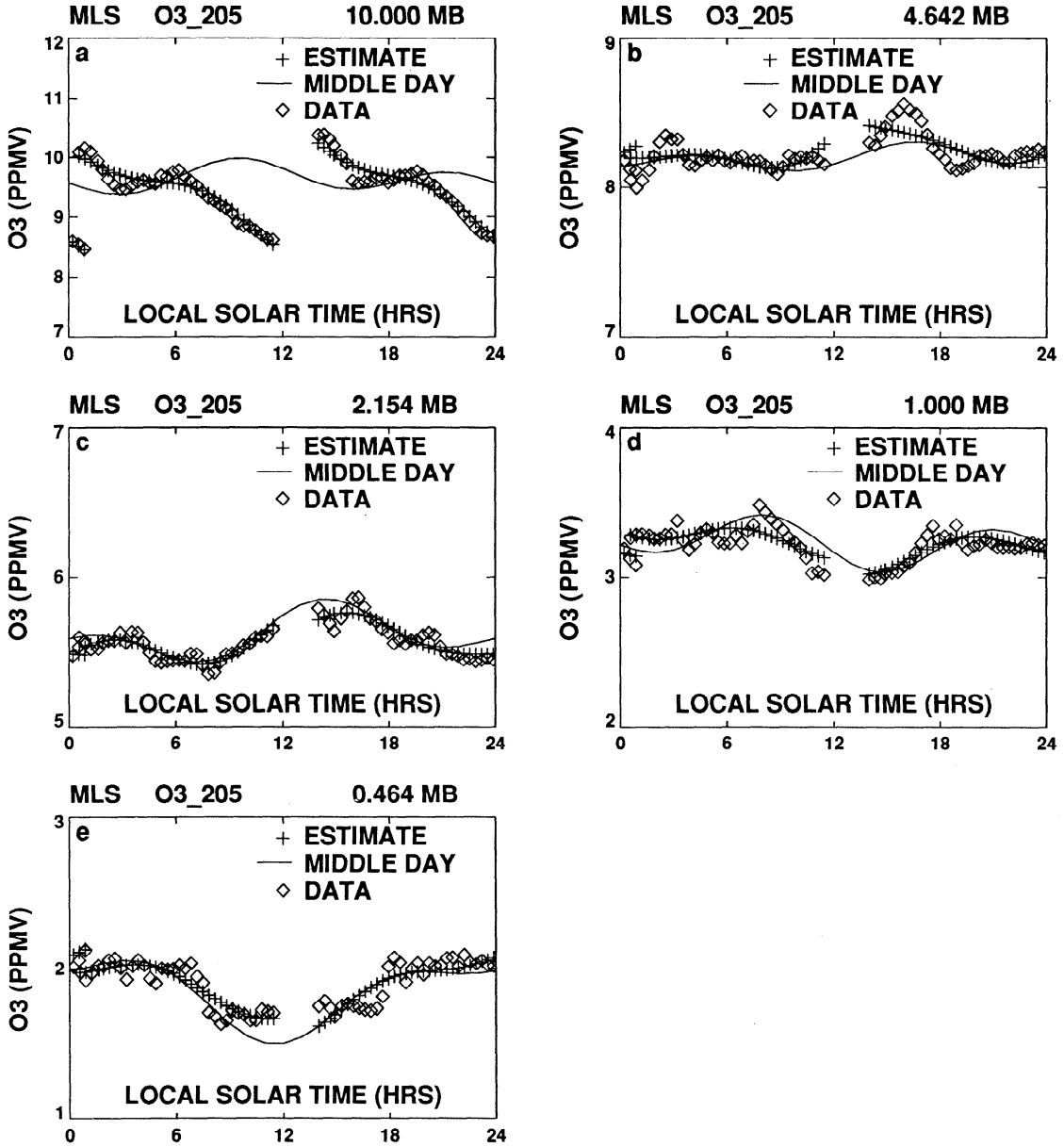

Figure 5. MLS O_3 zonal means as a function of local time at (a) 10.0 mbar, (b) 4.6 mbar, (c) 2.15 mbar, (d) 1.0 mbar, and (e) 0.46 mbar. As with Figure 4, the data correspond to the year-day period 92045-92085 (February 14 to March 25) at 28°N. In each of the plots, the diamonds denote the data, the pluses denote the values of the Fourier series evaluated at both the same day and the same local time of the corresponding data point, while the line represents the value of the estimate at various local times but for one day only, namely, year-day 92064 (March 4), which is near the midpoint of the yaw period.

3.3. Discussion of Results

Figures 5a-5e show the MLS zonal mean O_3 as a function of local time at 10.0, 4.6, 2.2, 1.0, and 0.46 mbar, respectively, for the period 92045-92085, at 28°N. In general, the Fourier estimates (pluses) match the data (diamonds) better when they are evaluated at both the same day and the local time of the data, compared with representing the diurnal variation only for day 92064 (line). Also, there are shorter-period phenomena in the data with periods of perhaps several days or more which are not reflected in our Fourier series estimate because, as noted earlier, the shortest period in day of year of the Fourier series is 36.5 days, and the shortest period in local time is 12 hours. Instead of extending the Fourier series to more terms, we analyze the shorter term phenomena in terms of residuals (the difference between the Fourier series estimate and the data). Figure 6 shows the residuals for ozone and temperature as a function of day at 2.2 mbar and 28°N for 1992. The variations in O_3 and temperature residuals do not appear to be purely random but appear to be anticorrelated to some degree. The correlation coefficient between the temperature and the O_3 residuals in Figure 6 is about -0.4, and the data for 1993 give similar results. The residuals in Figure 6 may be related to those observed by *Chandra* [1985], who analyzed ozone data from the backscatter ultraviolet (BUV) instrument and temperature data from the selective chopper radiometer (SCR), both on the Nimbus 4 satellite. For data at 2 mbar, Chandra found correlation coefficients between ozone

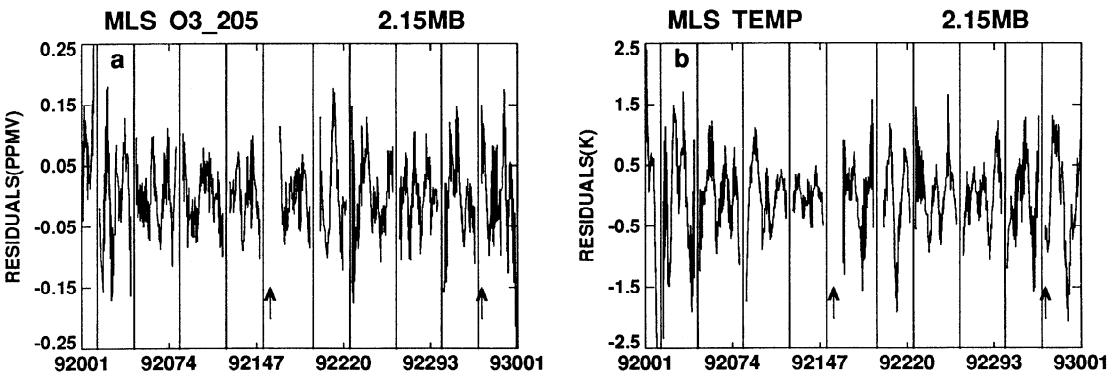

Figure 6. (a) MLS O_3 (ppmv) and (b) temperature (K) residuals as a function of day at 2.15 mbar and 28°N for 1992. The lines parallel to the ordinate denote the yaw days, and the larger data gaps in day of year are marked by vertical arrows.

and temperature residuals ranging from -0.6 (tropics) to -0.3 (high latitudes).

3.4. Estimation of Data Errors

In addition to the values of the individual data points, the L3AL data files also contain an estimated standard deviation for each data point. Although a very thorough and consistent analysis of errors of the MLS data is available [*Froidevaux et al.*, 1996; *Fishbein et al.*, 1996], the nature of the measurements complicates the situation. For example, MLS uses a priori information as well as atmospheric models of radiative transfer, both of which can introduce uncertainties. In addition to random errors associated with instrument noise, there may be systematic instrument errors, while the retrieval process (from telemetry to mixing ratios at a given location) could add some additional uncertainty. There may be additional uncertainty associated with ascending mode/descending mode differences. On the other hand, the procedure of calculating the diurnal and semidiurnal components from data over many days should reduce the effects of random error.

In order to provide some measure of goodness of fit, we consider in some detail the differences between the Fourier estimate and the data and their relation to uncertainties in the data. We will also consider estimates of uncertainties in the diurnal and semidiurnal coefficients. Details of the differences between the estimate and the data for 2.2 mbar, 28°N, and year 1992 have already been shown in Figure 6. An estimate of the standard deviation between the Fourier estimate and the data is given by the rms deviation

$$\text{rms} = \sqrt{\frac{1}{N-M}\sum_i (y_i - f_i)^2} \tag{1}$$

where the sum is over the number of data points N, M is the number of Fourier coefficients, and y_i and f_i are the data and the Fourier estimate, respectively.

An alternative estimate of quality, the reduced chi-square, is given by the expression

$$\chi_v^2 = \frac{1}{N-M}\sum_i (y_i - f_i)^2 / \sigma_i^2 \tag{2}$$

where σ_i^2 is the variance of the ith data point.

The rms values and reduced chi-square values corresponding to Figure 6 and other pressure levels are given in Table 1 for results based on data from 1992. Values and statistics at the intermediate levels (0.68, 1.5, 3.2 mbar) are based on MLS 3A data which were arrived at by using an averaging procedure of results from adjacent levels [*Froidevaux et al.*, 1996] and hence are not shown in Table 1. Column 3 of Table 1 gives the expectation values of the uncertainty (mean error) in the zonal means and are given by the expression

$$\overline{\sigma^2} = \left[\frac{1}{N}\sum_i \frac{1}{\sigma_i^2}\right]^{-1} \tag{3}$$

We have seen (Figure 6) that the values contributing to the rms are not purely random but are anticorrelated to the temperature differences. This may limit the interpretation of the chi-square values, but it also implies that information of variations smaller than the mean errors can be extracted. Although the reduced chi-square values do not indicate any problems, it is interesting to note that the rms values in Table 1 are all smaller than the corresponding mean errors of the zonal mean (column 3).

Table 2 gives the diurnal and semidiurnal amplitudes and phases averaged over the year, along with their uncertainties. The uncertainties are obtained from the covariance matrices of the two dimensional estimate and the rms differences. It should be noted that the use of the covariance matrix

Table 1. Statistics of Differences Between Data and Fourier Estimates at Representative Pressure Levels for 1992

Pressure mbar	Yearly Mean ppmv	Mean Error Zonal Mean ppmv	rms of Differences ppmv	Reduced Chi-Square
0.46	1.89	0.12	0.066	0.31
1.00	3.13	0.10	0.070	0.53
2.15	5.69	0.08	0.067	0.68
4.64	8.36	0.08	0.076	0.92

Table 2. Estimates of Amplitudes and Uncertainties in Diurnal and Semidiurnal Components Averaged Over 1992

Pressure mbar	Diurnal Amp Value ppmv	Diurnal Amp Error %	Diurnal Phase Value hours	Diurnal Phase Error	Semidiurnal Amp Value ppmv	Semidiurnal Amp Error %	Semidiurnal Phase Value hours	Semidiurnal Phase Error
0.46	0.20	14	0.3	0.5	0.06	24	6.6	0.6
1.00	0.11	20	2.2	1.0	0.09	20	7.9	0.6
2.15	0.10	17	14.9	1.4	0.01	24	5.3	0.7
4.64	0.10	21	15.2	1.1	0.03	27	1.9	0.7

implicitly assumes that the Fourier series expansion is an adequate model for the data (i.e., diurnal and semidiurnal components are sufficient). Therefore the values in Table 2 should be used only as an indication of the degree of errors. The values of the phase errors in Table 2 are generally overestimates. This is because sometimes the Fourier amplitudes are relatively small, in which case even small uncertainties in the amplitudes lead to large uncertainties in the phases (due to the nature of the inverse tangent function, from which the phases are calculated). Relatively small values of the amplitudes also could lead to relatively large percentage errors in the amplitudes. Although this situation is not the norm, they do contribute to the yearly average of the uncertainties in Table 2. For example, the majority of the uncertainties in the diurnal phase are between 0.5 and 1.1 hours. Table 3 gives amplitudes, phases, and corresponding errors for day 64 at standard pressures.

4. Description of the Photochemical Model

The photochemical model used is an improved version of that developed by *Pallister and Tuck* [1983] and *Austin* [1991]:the explicit model. Reaction rates and photochemical data have been taken from *DeMore et al.* [1994], while the photolysis scheme has been extended to a pressure of 0.01 mbar and has 61 levels between 1000 and 0.01 mbar inclusive. The model was run as a vertical stack of independent box models covering the UARS pressure levels 0.46 to 21.5 mbar. At each level the integration started close to sunset and was continued for 30 days, ensuring that the model reached photochemical equilibrium. The results presented refer to the diurnal variation calculated during the last day of the integration. The model was run at 28°N for days close to vernal equinox and the two solstices, and ending at day-of-year 64, 210, and 350. This gave results for almost the full range of solar declination experienced at this latitude.

The model was initialized with MLS O_3 data, Halogen Occultation Experiment (HALOE) data [*Russell et al.*, 1993], version 17, for H_2O, CH_4, HCl, NO_2, and NO and with model values for the remaining species. In addition, the observed diurnally varying MLS O_3 and temperature data, as deduced in section 3, were used for the computation of photolysis rates and for the thermal reaction rates, respectively. The model was initialized with zonally averaged HALOE data from day-of-year 57, 201, and 347, because of the unavailability of 28°N data for the above days. The differences in timing are small and are unlikely to influence the results significantly. HALOE data were chosen for initializing the model simulations because of their high precision and because of the improved simulations of upper stratospheric chemistry recorded by *Crutzen et al.* [1995] following their use.

5. Comparison Between Observations and Model Results

In comparing with the photochemical model calculations, the observations are based on data from September 1991 through October 1994 grouped into one 365-day period to avoid any interannual differences.

5.1. Comparison Between Absolute Values

For the latitude and days analyzed in this paper, MLS ozone data were generally larger than HALOE data throughout a significant part of the stratosphere (Figure 7), although in the mesosphere the difference between the observations decreased. It should be noted that a new version

Table 3. Estimated Uncertainties for Day 64, March 5

Pressure mbar	Diurnal Amp Value ppmv	Diurnal Amp Error %	Diurnal Phase Value hours	Diurnal Phase Error	Semidiurnal Amp Value ppmv	Semidiurnal Amp Error %	Semidiurnal Phase Value hours	Semidiurnal Phase Error
0.46	0.21	10	24.0	0.3	0.09	11	6.8	0.3
1.00	0.09	22	2.2	0.9	0.09	22	7.3	0.4
2.15	0.08	38	15.6	1.4	0.03	67	9.0	1.2
4.64	0.11	36	15.0	1.4	0.27	11	2.7	0.3

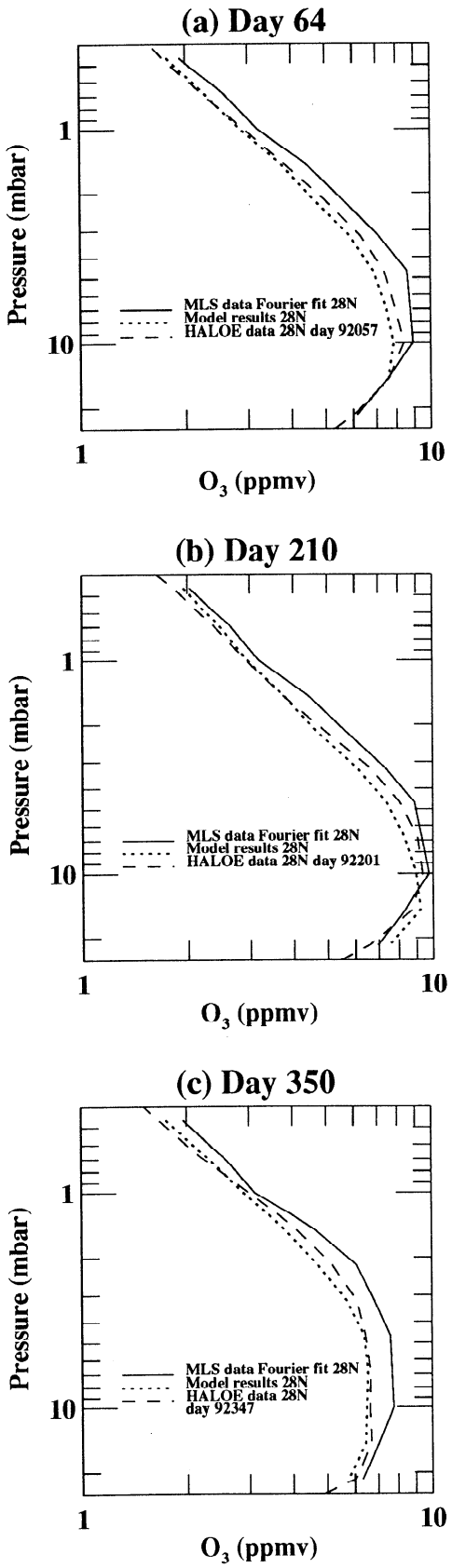

Figure 7. Zonal mean vertical ozone profile at 28°N on day 64 from MLS data using the diurnal variation algorithm in comparison with model results and HALOE data. (a) day 64 (March 5), (b) day 210, (c) day 350. Model results and MLS data have been taken at the same local time as the HALOE data.

of MLS data will soon become available and that the ozone mixing ratios are expected to decrease by up to 5% [*Waters*, 1996]. The results show features that have been well established by many previous modeling studies. For example, in the upper stratosphere and lower mesosphere the model underpredicts O_3 [e.g., *Eluszkiewicz and Allen*, 1993] relative to MLS data but is in agreement with HALOE data, within the errors of the measurements. Figure 7 also shows a region in which the model changes from underpredicting HALOE ozone slightly to overpredicting HALOE ozone slightly in the mesosphere. However, careful comparisons with observations are required because of the substantial diurnal variations at 1 mbar and above, as investigated in the next subsection.

The agreement between model results and HALOE data throughout the pressure range is consistent with the results of *Crutzen et al.* [1995]. Further analysis of their results using the current model suggests that their success arose largely from two factors, the specification of the correct HCl values (see also *Dessler et al.* [1996]) in the upper stratosphere and the fact that HALOE O_3 is typically smaller than other measurements. However, as noted by *Pallister and Tuck* [1983], the advantage of looking at diurnal variations is that these depend less on the absolute accuracy of the measurements but more on the relative variations which we explore in the next subsection.

5.2. Relative Diurnal Variations

Expressed as a percentage change from the midnight value, Figure 8 shows the photochemical model results for day 64 (dotted curves), the MLS Fourier analyzed observations (solid curves), and the chemical model results Fourier truncated to the same temporal resolution as the MLS data (dashed curves). At 10 mbar and below the model-simulated ozone diurnal variation was very small, about plus or minus 1%, while the neglect of transport has resulted in very poor agreement with the Fourier-analyzed observations. In contrast, in view of the error analysis noted above and the limited spectral resolution of the data, between 0.68 mbar and 3.2 mbar, the results are in very good agreement with the observations. In particular, the model simulated well the change in regime from a maximum in the afternoon at 3 mbar, to an intermediate state at 2.15 and 1.47 mbar with reduced diurnal variation, to the regime at 1 mbar and above with a minimum in the afternoon. At the top level, the results diverged significantly from the observations in that there was no indication in the observations of the temporary maximum simulated near local noon, although this feature disappeared for this day after Fourier truncation. The model results for day 210 (Figure 9), in general, showed poorer agreement with observations, particularly at 1 mbar and above. At 0.46 mbar the noon increase was considerably enhanced with relatively little sensitivity to day of year in the observations. At 3 mbar and below, agreement between model and observations was also poorer, with the observed variation larger than for day 64. Nonetheless, the qualitative features in the transition region near 2 mbar were again quite well reproduced. The model results for day 350 (Figure 10) were very similar to the results for day 64, but with improved mesospheric performance.

5.3. Comparison With Previous Results

5.3.1. Mesosphere. *Allen et al.* [1984] presented one of the earliest studies of the diurnal variations of ozone, which

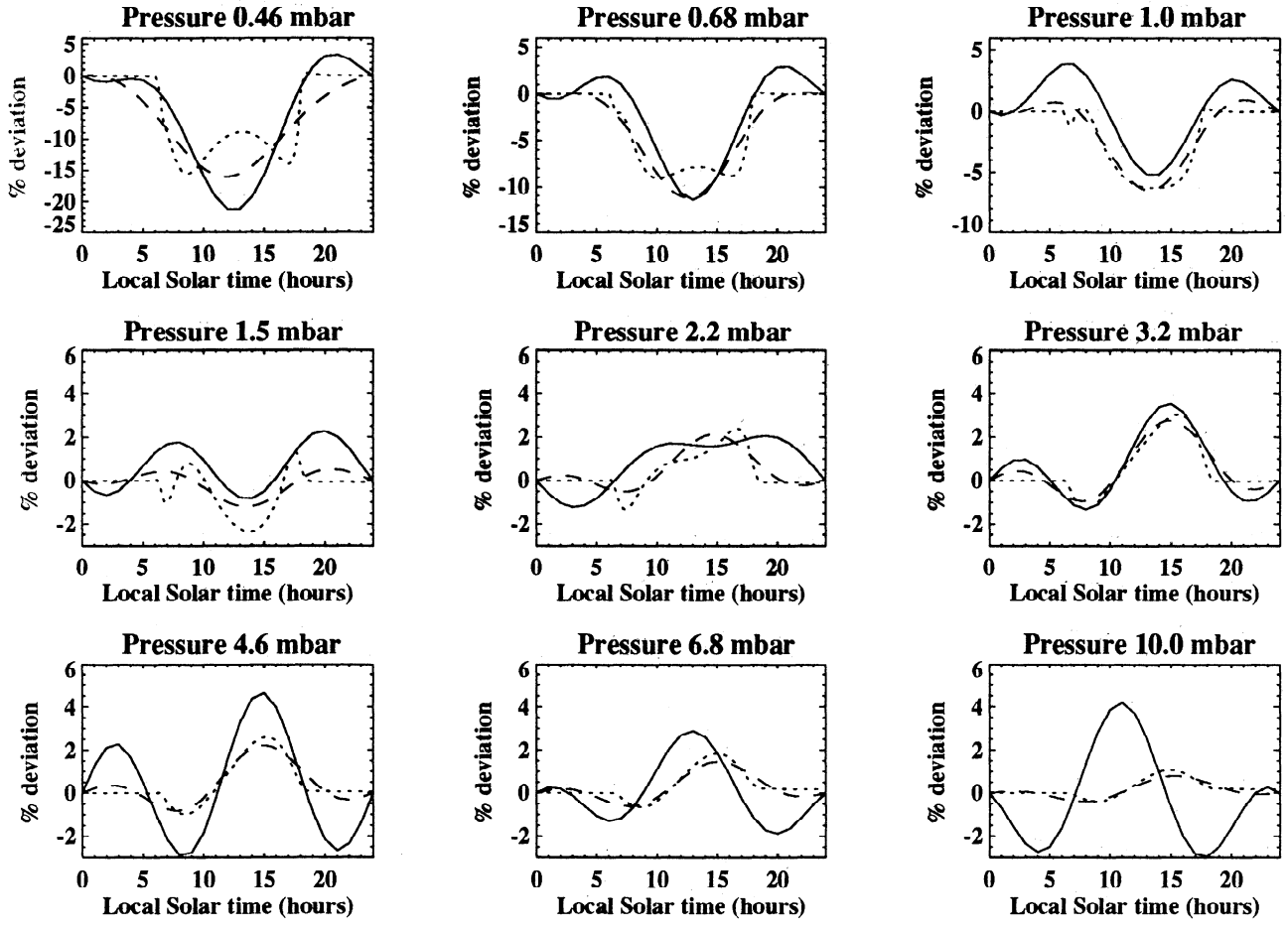

Figure 8. Diurnal variations of ozone at 28°N on day 64 on the pressure surfaces 0.46 to 10.0 mbar. Solid curve: MLS data using the diurnal variation algorithm; dotted curve: model results; dashed curve: model results truncated to the diurnal and semidiurnal components for more direct comparison with the MLS data.

showed that the diurnal variation depends largely on the ratio between the O_2 and the O_3 photolysis rates. Unfortunately, their results at 50 and 60 km do not show sufficient detail for comparison with the current work. *Connor et al.* [1994] show October results at 34°N indicating a minimum during the afternoon at 0.75 mbar, in agreement with the MLS data, with a value about 9% lower than at midnight. During March and December the afternoon reduction was slightly larger at 11%. This is in excellent agreement with the MLS data which show afternoon reductions of 10 to 12% on the days presented in this paper (see Figures 8-10).

The study by *Ricaud et al.* [1996], using MLS data from the 183-GHz channel, did not attempt to distinguish variations with day of year from diurnal variations. Instead, they analyzed data where the day-of-year variations are expected to be small (so that over a yaw period of about 36 days, variations are all attributed to behavior as a function of local solar time) and where the diurnal variations are greater than 10%. They have therefore restricted their analysis to altitudes between 0.46 mbar and 0.046 mbar. Their results, for October at 35°N and 0.46 mbar, indicate a smaller diurnal variation than the observations described here. *Ricaud et al.* [1996] also present results from two independent models, the Bordeaux and the Edinburgh models. Our results (Figure 8) are in good agreement with the former, and if anything, slightly closer to the MLS 183-GHz observations, which also confirm the ozone increase simulated near noon. In comparison, the Edinburgh model results are in poor agreement with observations in the lower mesosphere. The model neglects molecular scattering (R. Harwood, personal communication, 1996) because of its relative unimportance in the mesosphere in general, and this may have contributed significantly to the discrepancy with observations. Interestingly, earlier results of the Bordeaux model [*Ricaud et al.*, 1994] do not show a prominent maximum near noon.

5.3.2. Stratosphere. Despite a much larger solar declination the model results of *Bjarnason et al.* [1987] show the same qualitative features of an afternoon ozone increase of 6% peaking at about 3 mbar. At higher levels there is also a transition region and an afternoon ozone decrease in the lower mesosphere. Although concentrating on the mesosphere, *Connor et al.* [1994] also show results down to 3.2 mbar. Despite the instrument weighting function being averaged over a wide depth of atmosphere with different characteristics, their results show a midafternoon increase on some days, which peaks at about 4% in January, broadly consistent with MLS data. A much more quantitative comparison may be made with the results of *Pallister and Tuck* [1983] who present results between 40 and 48 km for equinox at 34°N, close to the latitude applicable to the results in Figure 8. At 48 km (approximately 1 mbar) a daytime maximum reduction of 6% was calculated in agreement with that found here, despite

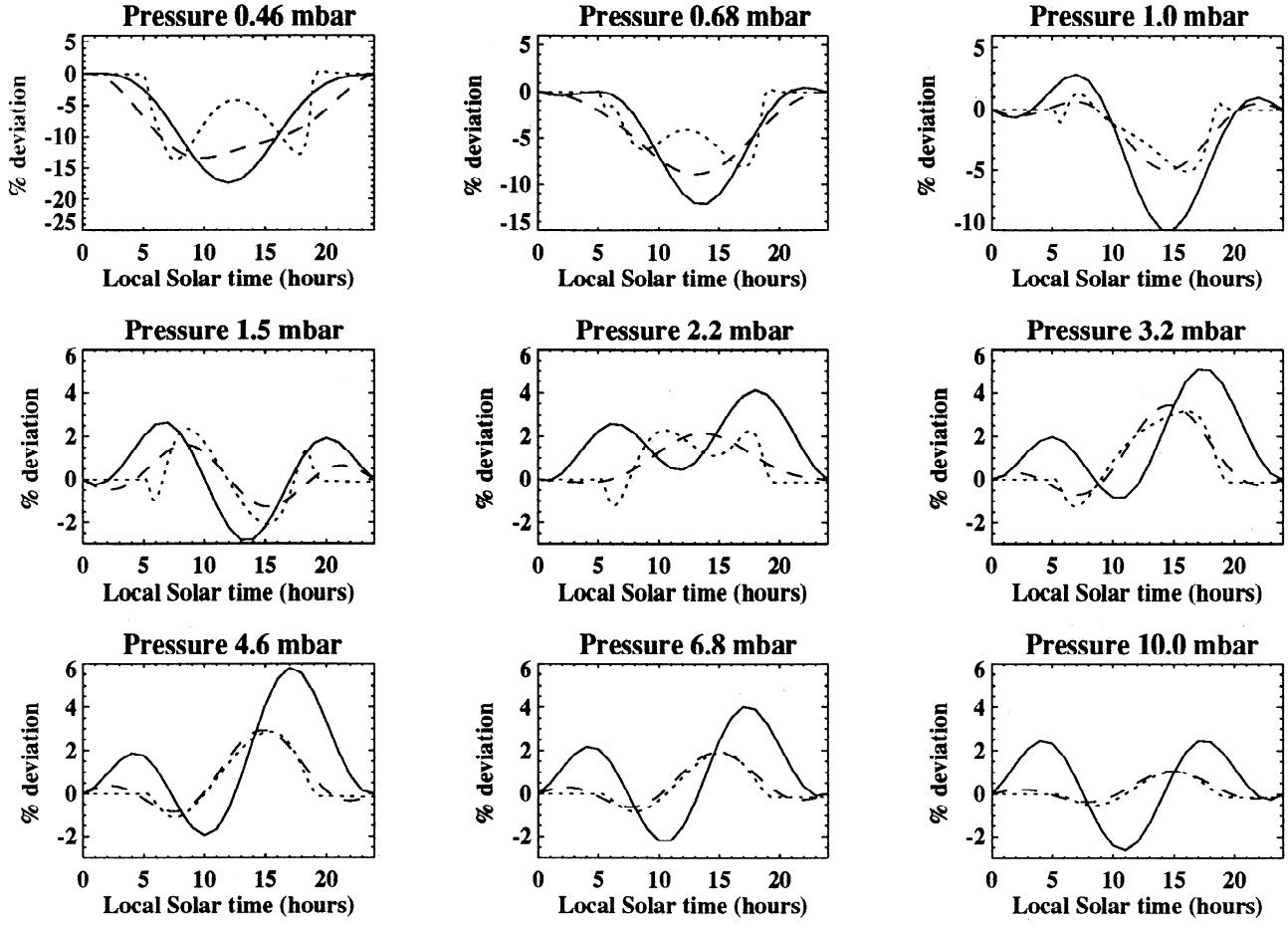

Figure 9. As Figure 8 but for day 210 (July 29).

numerous model and reaction rate changes in the last 10 years. Their results also show the transition region from low to high noon ozone values at altitudes of 44-46 km, about 2 km higher than in Figure 8. At 40 km (approximately 3 mbar) Pallister and Tuck calculated a peak midday value 4.5% above the midnight value compared with 3.1% in Figure 8. *Ricaud et al.* [1994] have also presented results from their photochemical model and compared them with ground-based microwave ozone measurements at 42 and 58 km over Bordeaux (45°N). Their model results are very similar but have a diurnal variation about 1% larger, which is in better agreement with our observations below the transition zone but slightly worse just above. However, the different latitude of their calculations (45°N) impedes direct comparison with our results.

6. Sensitivity of Model Results to Model Parameters

The model relative diurnal variation is insensitive to errors in the MLS and HALOE measurements. For example, a 10% change in NO_x affects the diurnal variation by up to 0.2% between 1.5 and 4.6 mbar. Similarly, a 10% change in the ozone profile used to compute the photolysis rates, affects the diurnal variation by less than 0.4% at 0.46 mbar, compared with the daytime reduction of 15%. Hence for conciseness, this section investigates the sensitivities of the diurnal variation due to other factors.

6.1. Tidal Effects

In the Pallister and Tuck results the ozone amount increased slightly during the night, particularly at 48 km. This is because of their use of eddy diffusion to mimic transport, whereas in our calculations transport has been neglected, and the daytime oxygen atoms react very rapidly with oxygen molecules at night so no nighttime change in ozone can occur. Nonetheless, some nighttime change in ozone was noted in the MLS observations presented in section 3, possibly due to tides, as noted by Pallister and Tuck. A qualitative appreciation of the effect of tides can be obtained by assuming that horizontal transport of ozone and temperature is negligible. It can be shown that

$$\frac{\partial [O_3]}{\partial t} = -\frac{\frac{1}{\kappa T}\left(\frac{\partial T}{\partial t} - J\right)\frac{\partial [O_3]}{\partial \ln p}}{\left(1 - \frac{1}{\kappa T}\frac{\partial T}{\partial \ln p}\right)} \quad (4)$$

where the left-hand side is the rate of change of the O_3 volume mixing ratio due to vertical transport, T is temperature, t is time, and p is pressure; κ is the gas constant divided by the specific heat at constant pressure, and J is the net diabatic heating. The vertical gradients of ozone and temperature and the rate of change of temperature were calculated from the MLS Fourier-analyzed data. Values for J were obtained using

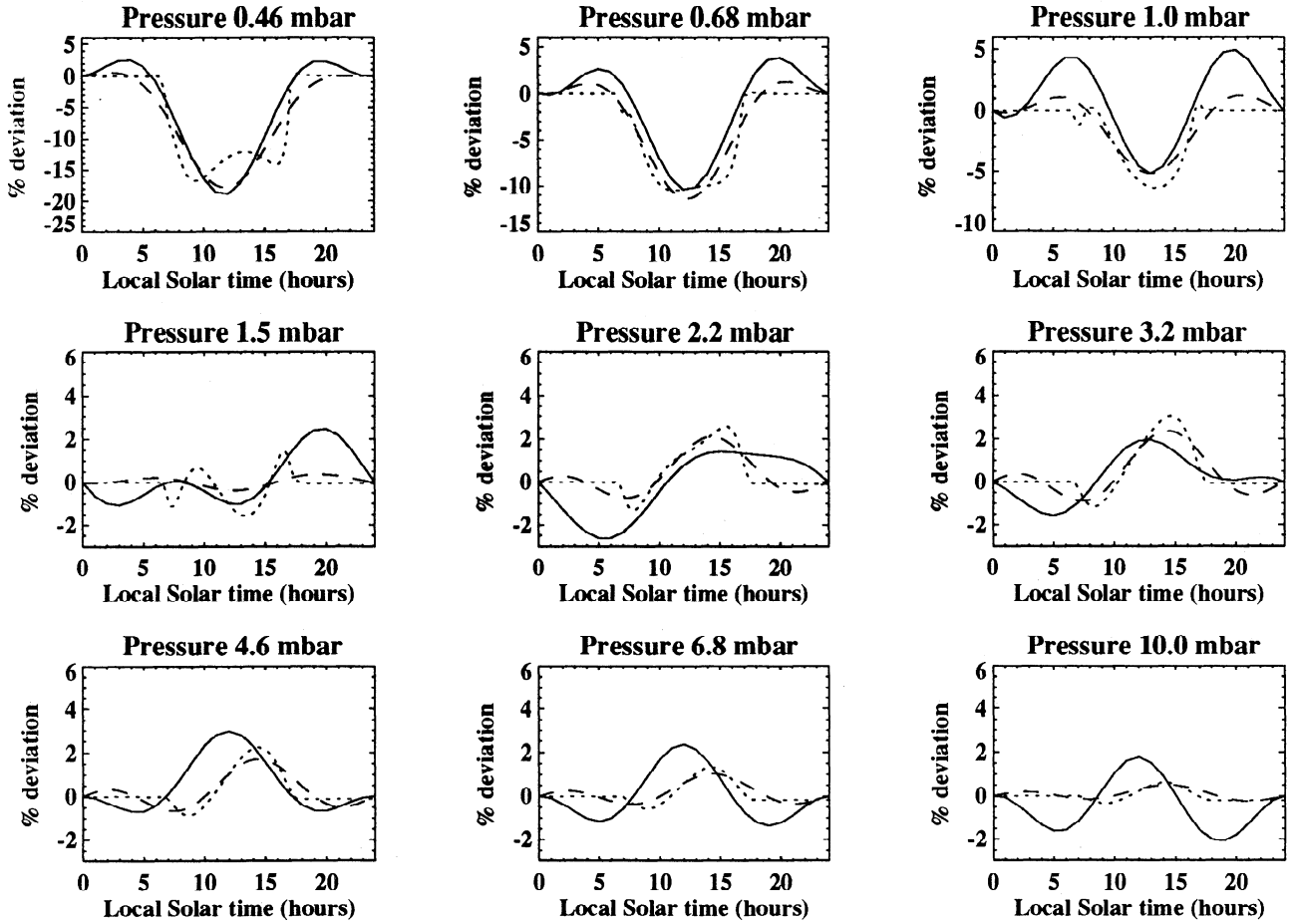

Figure 10. As Figure 8 but for day 350 (December 16).

the MIDRAD radiation scheme [*Shine*, 1987]. The ozone rate of change computed from equation (4) was then added to the photochemical change.

Comparisons of the calculated diurnal variation (Figure 11) with Figure 8 show that in the upper stratosphere and lower mesosphere the predawn ozone increase and postdusk ozone decrease were very well simulated. Between 1.5 and 4.6 mbar the amplitude of the diurnal variation increased, leading to an improvement at 4.6 and possibly 1.5 mbar but a general degradation in the other levels, particularly 2.2 mbar. In the middle stratosphere inclusion of tidal effects had a negligible effect on the results. Similar sensitivities to tidal effects were obtained for the other days investigated in this paper. To obtain good results in the transition region near 2 mbar is probably unrealistic using equation (4) since the diurnal variation is itself quite small, and the calculation of the ozone vertical gradient from observations with relatively poor vertical resolution is likely to introduce large errors. A thorough analysis of tidal effects would require the use of a tidal model, which is beyond the scope of the current work.

6.2. Thermal Reaction Rates

Figure 12 shows the results obtained for the diurnal variation assuming only the Chapman reactions for oxygen species with the other reactions in the model switched off. Broadly, the same diurnal variation was obtained, as shown in Figure 11, but with an enhanced variation at 0.46 mbar and a somewhat reduced amplitude for the variation below 1 mbar. Thus, in contrast to the Pallister and Tuck conclusions, these results show that the transition region near 2 mbar is largely due to oxygen photochemistry. Near 3 mbar, NO_x chemistry enhances the late afternoon peak with HO_x chemistry playing a minor role. The model sensitivity to the following rate limiting steps was therefore investigated by performing model calculations for day 64 with the rates decreased by the error bars in the work of *DeMore et al.* [1994]:

(R1) $O + HO_2 \rightarrow OH + O_2$

(R2) $O + NO_2 \rightarrow NO + O_2$

At 1 mbar the daytime ozone diurnal variation changed by typically less than 0.05% due to the change in the rate for (R1). Between 1.5 and 4.6 mbar the afternoon peak decreased by between 0.2 and 0.4%, primarily due to (R1) higher up and (R2) lower down. This resulted in slightly better agreement with observations at 3.2 mbar and above but slightly worse agreement at 4.6 mbar.

6.3. Photolysis Reaction Rates

During the daytime in the lower mesosphere, ozone is initially photolyzed, but later, O_2 photolysis increases odd oxygen which in turn increases ozone toward noon. During

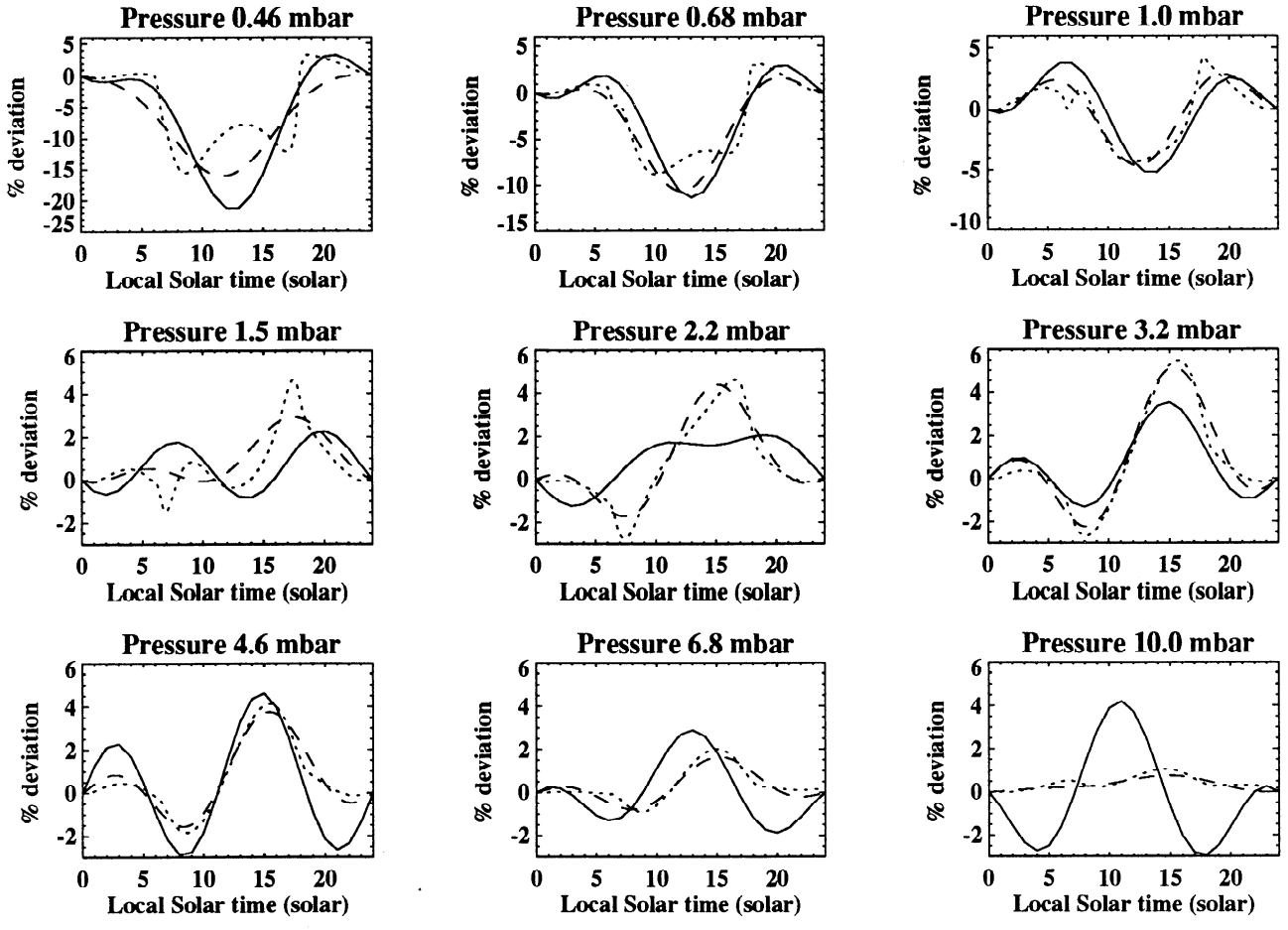

Figure 11. As Figure 8 but including a simplified representation of vertical transport (see equation (4)).

the afternoon, O_2 photolysis starts to reduce again, and consequently, the ozone amount also reduces. Finally, toward sunset all the oxygen atoms recombine to form ozone. Consequently, some sensitivity of the results to photolysis rate parameters would be expected. In particular, increasing the O_3 absorption cross sections by 10%, the suggested error bar, in *DeMore et al.* [1994], reduced the ozone amount throughout the stratosphere and lower mesosphere by between about 5% and 10%. At 0.46 mbar this change increased the maximum daytime reduction from 15.5% to 16.6%, slightly closer to that observed. When vertical transport was included, the diurnal variation at 1 mbar was also improved slightly with a daytime reduction changing from 4.4% to 5.0% compared with the observed 5.2 ± 0.8% reduction. Below the transition zone, the percentage change from the midnight value increased by about 0.4% during the afternoon, thus giving poorer agreement with observations at 2.2 and 3.2 mbar but better agreement at 4.6 mbar (see Figure 13 which also includes reductions in the rates for (R1) and (R2)).

A uniform 20% increase in the O_2 cross sections, the suggested error bar of DeMore et al. [1994], increased the ozone amount at midnight by 8-9% between 4.6 and 0.46 mbar. At 0.46 mbar the maximum daytime reduction changed by less than 0.1%, but in the early afternoon, the reduction from the midnight value was about 1.2% higher. Further model results have shown that in the lower mesosphere the daytime model O_3 peak is caused by the Schumann-Runge (*S-R*) bands. Therefore the magnitude of the peak could be sensitive to the precise treatment of the bands, which here follows *Allen and Frederick* [1982] with updated values for the *S-R* continuum. At 1 mbar and below, the adjustment in the O_2 cross sections changed the diurnal variation by typically less than 0.1%.

6.4. Net Effect of Reaction Rate Changes on Absolute Ozone Amounts

Ideally, one would like to be able to suggest reaction rate changes which can consistently improve both the ozone diurnal variation and the absolute ozone amounts in comparison with observations. The reduction in the rates for (R1) and (R2) increased ozone in the upper stratosphere more in agreement with MLS data (Figure 14, run b; compare run a which assumes the recommended rates). *Clancy et al.* [1994] also found significant improvements in the modeling of upper stratospheric ozone (and HO_2) when the rate for (R1) was reduced. While an increase in O_3 cross sections improves the lower mesospheric ozone diurnal variation, the absolute values are adversely affected, as noted in section 6.3. However, these changes, combined with an increase in the O_2 cross sections can result in an overall improvement in the results, as indicated in Figure 14, run c.

7. Summary and Conclusions

Two-dimensional Fourier series estimates of MLS ozone data from the UARS have been obtained to describe local time

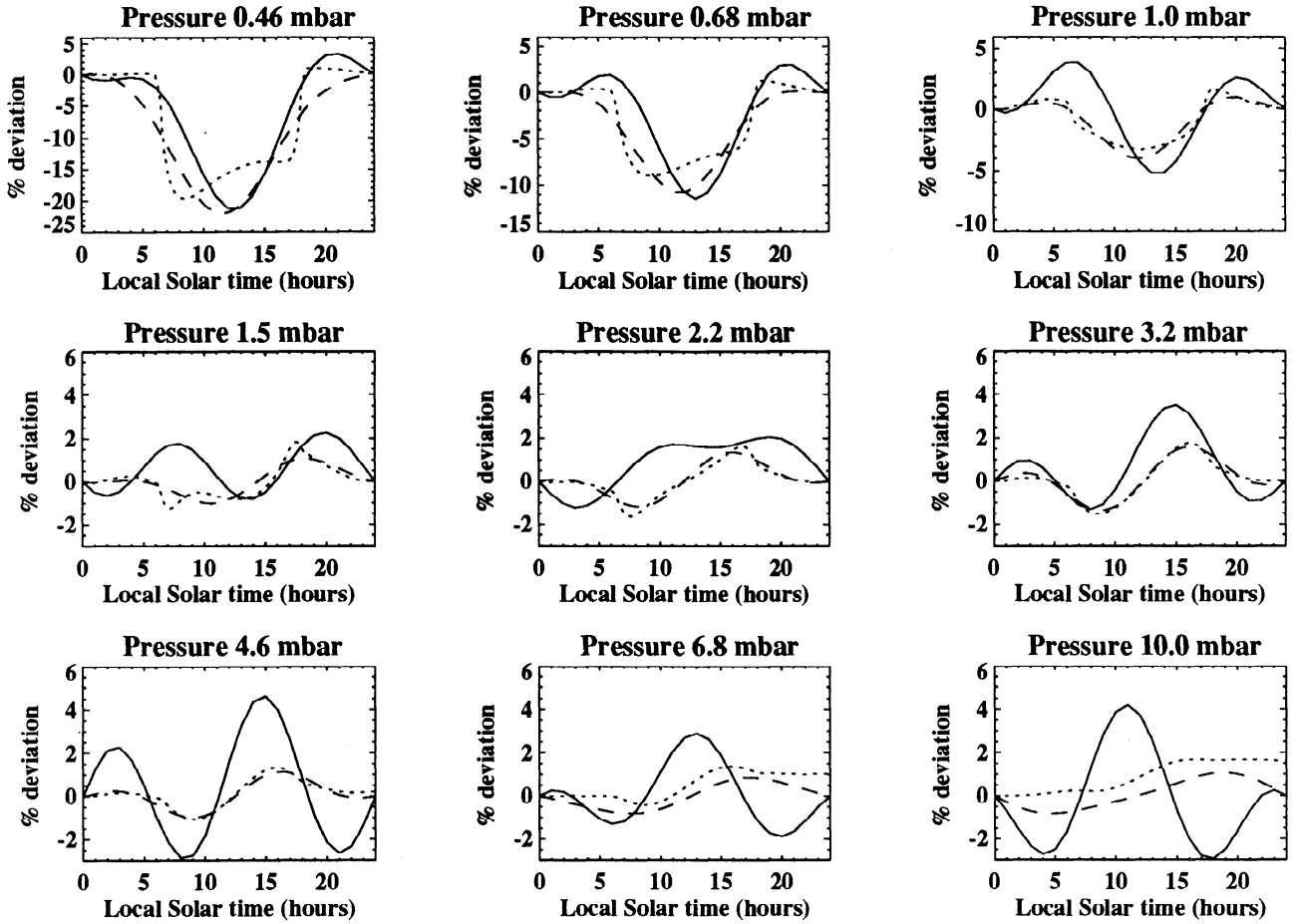

Figure 12. As Figure 11 but assuming only oxygen chemistry in the model.

and annual variations in the middle and upper stratosphere. Major considerations in the data analysis include constraints imposed by the sampling of the data and the relatively small magnitudes of the diurnal variations. Because of these small changes, care must be taken in relation to measurement uncertainties, and no averaging of the zonal mean data was performed in the analysis. The residuals between the data and the diurnal variation estimate compare favorably with studies of planetary oscillations of ozone and temperature [*Chandra*, 1985] based on data from the Nimbus 4 satellite. The Nimbus 4 measurements were Sun synchronous and did not extend to diurnal variations. This lends support that our results have identified diurnal variations reasonably. In addition to being able to analyze relatively small variations, the method of analysis expounded in this paper can be applied to UARS data generally, and similar results to that shown above can be generated between latitudes 32°N and 32°S for each day of the year. Possible extensions of the method would allow diurnal variations to be deduced at higher latitudes, again throughout the year and throughout the same pressure range. Previously, data have often been restricted to day-night differences from satellites, or full diurnal variations, but only at a single fixed location. Despite these strengths with the current analyses, the model calculations have shown that the truncation of the diurnal variation to the diurnal and semidiurnal components may lead to significant differences from the actual diurnal variations of ozone, particularly in the lower mesosphere. The observations from the MLS instrument are broadly consistent with a variety of other measurements from different instruments [e.g., *Connor et al.*, 1994, *Ricaud et al.*, 1996, *Bjarnason et al.*, 1987].

The diurnal variation of ozone was found to be broadly similar throughout the year. At 3 mbar, ozone reaches a maximum in the afternoon, some 4% higher than at midnight, while at 1 mbar ozone is a minimum in the afternoon, some 5% lower than at midnight. Between these pressures there is a transition region where the deviation from the midnight value drops to 2% or less. Above 1 mbar, ozone is lower during the day, and the percentage deviation from the midnight value increases with height and may exceed 20% at 0.46 mbar, depending on the time of year.

For currently recommended reaction rates [*DeMore et al.*, 1994], photochemical model simulations agreed well with the observations with respect to the relative variation and were in quite good agreement with calculations of *Ricaud et al.* [1994] and *Pallister and Tuck* [1983], despite more than 10 years of reaction rate changes since the latter study. However, some systematic errors were present relative to MLS data, primarily the well-established underprediction of upper stratospheric and lower mesospheric ozone. The model relative diurnal variation was found to be sensitive to a number of parameters, particularly vertical transport. This sensitivity was particularly enhanced in the transition region, possibly because of oversimplifications in representing the transport terms. The main difference between the MLS 205-GHz measurements and the model diurnal variation was an

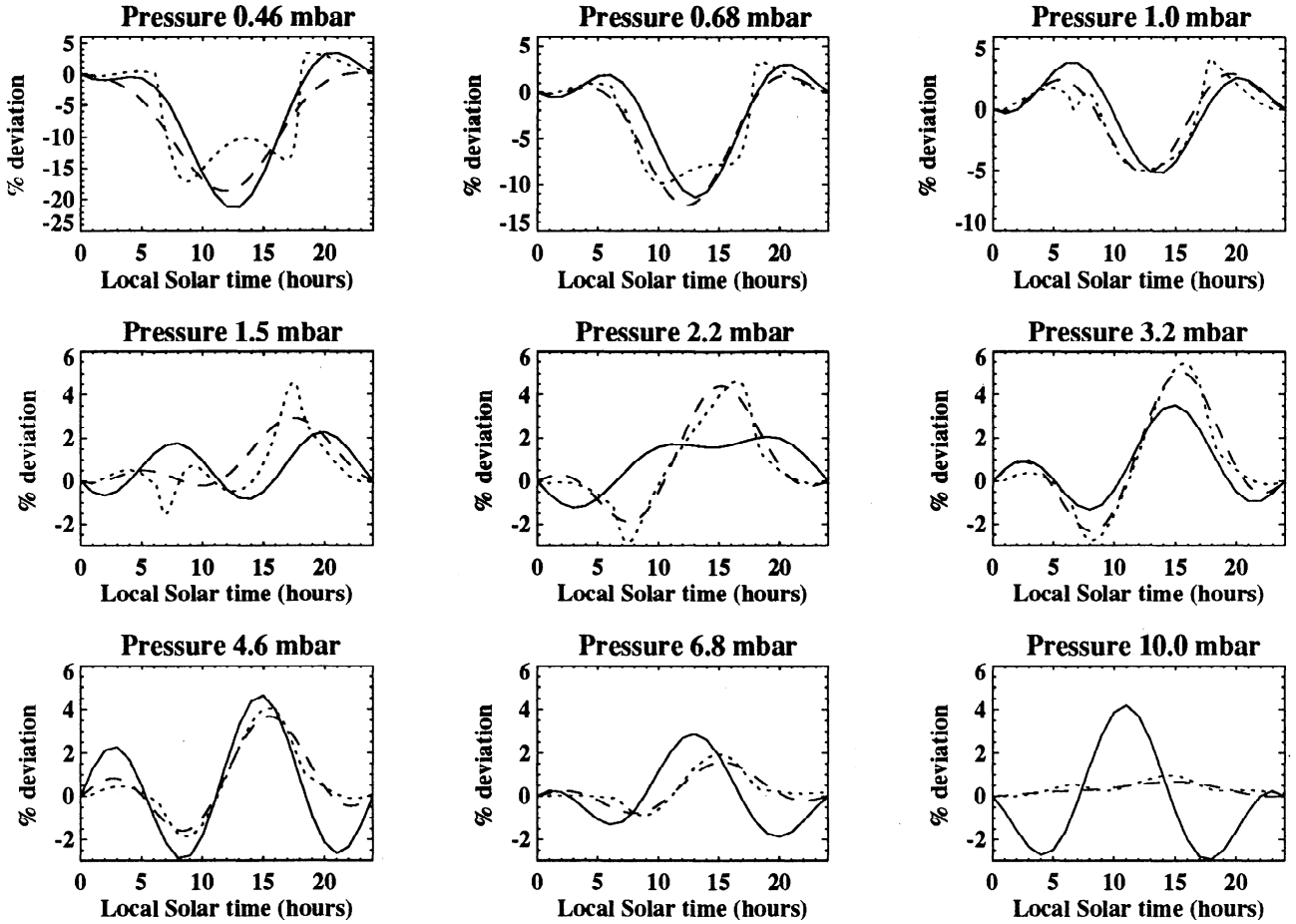

Figure 13. As Figure 11 but with the rates for the reactions $O + HO_2 \rightarrow OH + O_2$ and $NO_2 + O \rightarrow NO + O_2$ decreased to their measured limits and the ozone absorption cross-sections increased by 10%.

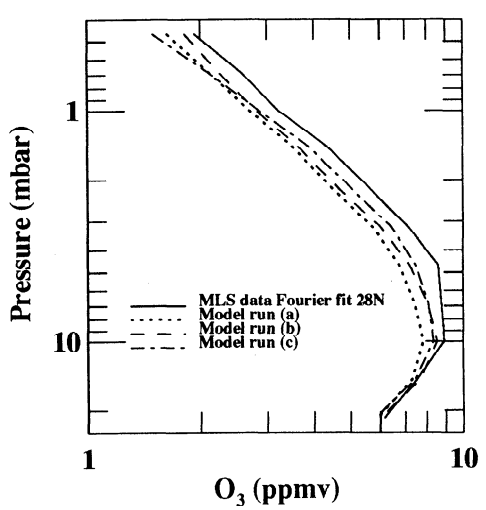

Figure 14. As Figure 7a but including vertical transport (equation (4)) and changes to model parameters as follows: run a recommended rates for (R1) and (R2); run b rates for (R1) and (R2) decreased to their lower limits; run c rates for (R1) and (R2) decreased to their lower limits, ozone crosssections increased by 10% and O_2 cross sections increased by 20%.

insufficient percentage ozone reduction during the daytime at the top level considered (0.46 mbar). However, comparisons were very favorable with results from the alternative 183-GHz MLS ozone channel [*Ricaud et al.*, 1996]. We have found that the 183-GHz radiometer results are less noisy than the corresponding retrievals from the 205-GHz radiometer at 0.46 mbar and may produce more accurate results at this level [but see, e.g., *Froidevaux et al.*, 1996]. Some sensitivity of the results was also found to the O_2 and O_3 cross sections and to the rates of the thermal reactions

$$O + HO_2 \rightarrow OH + O_2$$

$$O_3 + HO_2 \rightarrow OH + 2O_2$$

$$O + NO_2 \rightarrow NO + O_2$$

The results of changing the rate for the second reaction were not shown here, because of their similarity with the effects of the first reaction. Reduction of the rates to the lowest values currently recommended [*DeMore et al.*, 1994], together with increases in the O_2 and O_3 cross sections, could help resolve the model underprediction of ozone and improve the modeled ozone relative diurnal variation. However, errors in the measured diurnal variations prevent more definite conclusions

to be made. Nonetheless, the further laboratory investigation of the above reaction rates and cross sections could prove valuable in resolving the remaining discrepancies between model and observations. Comparisons between the results of different photolysis schemes could also be beneficial because of the sensitivity of the results to O_3 and O_2 photolysis rates. Further evaluation of observations as a function of latitude could also aid the comparisons with models, but this was beyond the scope of the current work.

Acknowledgments. We thank J. W. Waters and the MLS team. Thanks also go to two reviewers for their insightful comments. The work by FTH was supported by NASA under contract NAS5-31752.

References

Allen, M., and J.E. Frederick, Effective dissociation cross-sections for molecular oxygen and nitric oxide in the Schumann-Runge bands, *J. Atmos. Sci., 39*, 2066-2075, 1982.

Allen, M., J.I. Lunine, and Y.L. Yung, The vertical distribution of ozone in the mesosphere and lower thermosphere, *J. Geophys. Res., 96*, 4841-4872, 1984.

Austin, J., On the explicit versus family solution of the fully diurnal photochemical equations of the stratosphere, *J. Geophys. Res., 96*, 12,941-12,974, 1991.

Barth, C.A., D.W. Rusch, R.J. Thomas, G.H. Mount, G.J. Rottmon, G.E. Thomas, R.W. Saunders, and G.M. Lawrence, Solar Mesosphere Explorer : Scientific objectives and results, *Geophys. Res. Lett., 10*, 237-240, 1983.

Barath, F.T., et al., The Upper Atmosphere Research Satellite Microwave Limb Sounder 94, *J. Geophys. Res., 98*, 10,751-10,762, 1993.

Bjarnason, G.G., S. Solomon, and R.R. Garcia, Tidal influences on vertical diffusion and diurnal variability of ozone in the mesosphere, *J. Geophys. Res., 92*, 5609-5620, 1987.

Chandra, S., Solar induced oscillations in the stratosphere: A myth or reality?, *J. Geophys. Res., 90*, 2331-2339, 1985.

Clancy, R.T., D.W. Rusch, R.J. Thomas, M. Allen, and R.S. Eckman, Model ozone photochemistry on the basis of Solar Mesosphere Explorer mesospheric observations, *J. Geophys. Res., 92*, 3067-3080, 1987.

Clancy, R.T., B.J. Sandor, D.W. Rusch, and D.O. Muhleman, Microwave observations and modeling of O_3, H_2O, and HO_2 in the mesosphere, *J. Geophys. Res., 99*, 5465-5473, 1994.

Connor, B.J., D.E. Siskind, J.J. Tsou, A. Parrish, and E. E. Remsberg, Ground-based microwave observations of ozone in the upper stratosphere and mesosphere, *J. Geophys. Res.*, 99, 16,757-16,770, 1994.

Crutzen, P.J., J.-U. Grooss, C. Bruhl, R. Muller, and J.M. Russell III, A reevaluation of the ozone budget with HALOE UARS data: No evidence for the ozone deficit, *Science, 268*, 705-708, 1995.

DeMore, W.B., S.P. Sander, C.J. Howard, A.R. Ravishankara, D.M. Golden, C.E. Kolb, R.F. Hampson, M.J. Kurylo, and M.J. Molina, Chemical kinetics and photochemical data for use in stratospheric modeling, in *Evaluation 11, JPL 94-26*, Jet Propul. Lab., Calif. Inst. Technol., Pasadena, Ca., 1994.

Dessler, A.E., S.R. Kawa, D.B. Considine, J.W. Waters, L. Froidevaux, and J.B. Kumer, UARS measurements of ClO and NO_2 at 40 and 46 km and implications for the model "ozone deficit", *Geophys. Res. Lett.*, 23, 339-342, 1996.

Eluszkiewicz, J. and M. Allen, A global analysis of the ozone deficit in the upper stratosphere and lower mesosphere, *J. Geophys. Res., 98*, 1069-1082, 1993.

Fishbein, E. F., et al., Validation of UARS Microwave Limb Sounder temperature and pressure measurements, *J. Geophys. Res., 101*, 9983-10,016, 1996.

Froidevaux, L., et al., Validation of UARS Microwave Limb Sounder ozone measurements, *J. Geophys. Res., 101*, 10,017-10,060, 1996.

Gille, J.C., and J.M. Russell III, The Limb Infrared Monitor of the Stratosphere (LIMS): Experiment description, performance and results, *J. Geophys. Res., 89*, 5125-5140, 1984.

Huang, F. T., P. B. Hays, and C. A., Reber, Retrieval of local solar time information in atmospheric measurements from the Upper Atmosphere Research Satellite, *EOS Trans.* AGU, Spring Meet. Suppl., 75(16), 84, 1994.

Kondo, Y., P. Aimedieu, M. Pirre, W.A. Matthews, R.A. Ramaroson, W.R. Sheldon, J.R. Benbrook, and A. Iwata, Diurnal variation of nitric oxide in the upper stratosphere, *J. Geophys. Res., 95*, 22,513-22,522, 1990.

Pallister, R.C., and A. F. Tuck, The diurnal variation of ozone in the upper stratosphere as a test of photochemical theory, *Q. J. R. Meteorol. Soc., 109*, 271-284, 1983.

Reber, C.A., The Upper Atmosphere Research Satellite (UARS), *Geophys. Res. Lett, 20*, 1215-1218, 1993.

Reber, C. A., C. E. Trevathan, R. J. McNeal, and M. R. Luther, The Upper Atmosphere Research Satellite (UARS) Mission, *J. Geophys. Res., 98*, 10,643-10,647, 1993.

Reber, C. A., R.S. Stolarski, L. Froidevaux, E. F. Fishbein, J. W. Waters, A.E. Roche, and F. T. Huang, Local solar time effects on equatorial stratospheric temperatures and ozone from UARS, *EOS Trans, 75 (16)*, AGU Spring Suppl., 95, 1994.

Ricaud, P., J. de La Noe, B. J. Connor, L. Froidevaux, J. W. Waters, R. S. Harwood, I. A. Mackenzie, and G. E. Peckham, Diurnal variability of mesospheric ozone as measured by the UARS microwave limb sounder instrument: Theoretical and ground-based validations, *J. Geophys Res., 101*, 10,077-10,089, 1996.

Ricaud, P., G. Brasseur, J. Brillet, J. de La Noe, J. P. Parisot, and M. Pirre, Theoretical validation of ground-based microwave ozone measurements, *Ann. Geophys., 12*, 664-673, 1994.

Russell, J.M., III, L.L. Gordley, J.H. Park, S.R. Drayson, W.D. Hesketh, R.J. Cicerone, A.F. Tuck, J.E. Frederick, J.E. Harries, and P.J. Crutzen, The Halogen Occultation Experiment, *J. Geophys. Res., 98*, 10,777-10,797, 1993.

Shine, K.P., The middle atmosphere in the absence of dynamical heat fluxes, *Q. J. R. Meteorol. Soc., 113*, 603-633, 1987.

Siskind, D.E., E.E. Remsberg, R.S. Eckman, and B.J. Connor, Model/data comparisons of ozone in the upper stratosphere and mesosphere, in *Proceedings of the Quadrennial Ozone Symposium*, edited by R.D. Hudson, *NASA Conf. Publ. 3266*, pp. 294-297, 1994.

Waters, J. W., Microwave Limb Sounding, chap. 8 in *Atmospheric Remote Sensing by Microwave Radiometry*, edited by M.A., Janssen, John Wiley, New York, 1993.

Waters, J. W., MLS instrument and data processing update paper, presented at the UARS Science Team Meeting, NASA/LaRC, 26-28 March, 1996.

Webster, C.R., and R.F. May, Simultaneous in situ measurements and diurnal variations of NO, NO_2, O_3, N_2O, CH_4, H_2O, and CO_2 in the 40- to 26-km region using an open path tunable diode laser, *J. Geophys. Res., 92*, 11,931-11,950, 1987.

Webster, C.R., R.F. May, R. Toumi and J.A. Pyle, Active nitrogen partitioning and the nighttime formation of N_2O_5 in the stratosphere: simultaneous in situ measurements of NO, NO_2, HNO_3, O_3, and N_2O using the BLISS diode laser spectrometer, *J. Geophys. Res., 95*, 13,851-13,866, 1990.

Zommerfelds, W.C., K.F. Kunzi, M.E. Summers, R.M. Bevilacqua, D.F. Strobel, M. Allen, and W.J. Sawchuk, Diurnal variations of mesospheric ozone obtained by ground-based microwave radiometry, *J. Geophys. Res., 94*, 12,819-12,832, 1989.

John Austin, UK Meteorological Office, London Rd., Bracknell, Berks RG12 2SZ, UK. (e-mail: jaustin@meto.gov.uk)

Frank T. Huang, Science Systems and Applications Inc., 5900 Princess Garden Parkway, Lanham, Md. 20706. (e-mail: huang@grid.gsfc.nasa.gov)

Carl A. Reber, NASA Goddard Space Flight Center, Greenbelt Md., 20771. (e-mail: reber@skip.gsfc.nasa.gov)

(Received September 20, 1996; revised January 16, 1997; accepted February 8, 1997.)